

Superhard phase composed of single-wall carbon nanotubes

M. Popov,¹ M. Kyotani,¹ R. J. Nemanich,² and Y. Koga^{1,3}

¹*Joint Research Consortium of Frontier Carbon Technology, JFCC, c/o AIST, Tsukuba Central 5, 1-1-1 Higashi, Tsukuba, Ibaraki 305-8565, Japan*

²*Department of Physics, North Carolina State University, 408A Cox, Box 8202, Raleigh, North Carolina, 27695-8202*

³*Research Center for Advanced Carbon Materials, National Institute of Advanced Industrial Science and Technology (AIST), Tsukuba Central 5, 1-1-1 Higashi, Tsukuba, Ibaraki 305-8565, Japan*

(Received 27 April 2001; revised manuscript received 13 July 2001; published 2 January 2002)

Single-wall carbon nanotubes (SWNT's) have been studied under pressure up to 55 GPa. We report experimental data on irreversible changes of mechanical and structure properties of SWNT under pressure. The new superhard phase (SP-SWNT) composed of single-wall carbon nanotubes has been studied which exhibits a bulk modulus exceeding or comparable with diamond and hardness belongs to the range between cubic BN and diamond. The SP-SWNT were synthesized by applying a shear deformation under load in a diamond-anvil cell; the procedure of stress tensor variation. After intermediate phase transitions, single-wall carbon nanotubes are transformed to SP-SWNT at pressure of 24 GPa. The transformation is accompanied by irreversible changes in the Raman spectra. The nanotubes do not collapse at least up to pressure 55 GPa (maximum pressure of the study). Bulk modulus of 462 to 546 GPa was found out for SP-SWNT from the comparative study of pressure dependence of the Raman modes of SP-SWNT (high-energy mode $\sim 1590\text{ cm}^{-1}$) and diamond (1333 cm^{-1}). This value exceeds the bulk modulus of diamond (420 GPa for single diamond crystal). Hardness measurements were performed using nanoindentation technique. Hardness of SP-SWNT (62 to 150 GPa) was found out from comparative study of SP-SWNT, diamond and cubic BN.

DOI: 10.1103/PhysRevB.65.033408

PACS number(s): 61.46.+w, 81.40.Vw, 78.30.Na, 62.20.Dc

Theoretical and experimental studies give the value of Young's modulus for single-wall carbon nanotubes (SWNT) (Ref. 1) in the tera-Pascal range (Refs. 2 and 3). Capability of carbon for the forming of sp^3 bonding between curved graphite (sp^2 bonded) sheets (Refs. 4–10) provides a possibility for creation of superhard carbon nanocluster-based materials. Polymerization of nanotubes via sp^3 bonding and possible structures were studied theoretically in Ref. 4. SP-SWNT with sp^3 intertube bonding are expected to have highly anisotropic mechanical and electrical (metallic and semiconductor) properties while exhibiting superhard material characteristics.

Under hydrostatic conditions graphite does not transform to diamond at least up to 80 GPa,¹¹ while stress tensor variation (by applying shear deformation under load) leads to direct transformation of graphite to diamond at a pressure of 17 GPa at room temperature.¹² Success in ultrahard fullerite synthesis at 18 GPa at room temperature using stress tensor variation in a shear diamond anvil cell (SDAC) demonstrates the advantages of this procedure.⁵ In the present study the same procedure was successfully applied for synthesis of SP-SWNT.

The SWNT bundles used in this study were obtained from Tubes@Rice (Rice University in Houston, TX). The nanotubes are composed of a nearly random mixture of arm-chair, zig-zag, and chiral helicities. The mean tube diameter of 1.2 nm is obtained by the manufacturing procedure¹³ and is appropriate for our Raman measurements.

In SDAC controlled shear deformation is applied to a specimen under pressure by rotation of one of the anvils around an axis of load. The application of shear deformation (stress tensor variation) decreases the hysteresis of a phase transformation and makes it possible to obtain a homoge-

neous phase (see, for example, Ref. 5, and references therein). At the phase transition, a steplike anomaly of the radial pressure distribution in the sample (due to volume and elastic modulus jump) appears for the case of nonhydrostatic compression. According to the procedure described in Ref. 5, these anomalies were detected for pressures of 14 ± 1 , 19 ± 1 , and 24 ± 1 GPa. The pressure was measured by the ruby-fluorescence procedure. Ruby particles ($1\text{--}3\ \mu\text{m}$ in size) were deposited onto the working surface of the diamond anvil. Specimens were loaded in the gasket without a pressure medium.

The sample state while under pressure was registered by Raman scattering. The Raman spectra were recorded using a Jasco NRS-2100 triple mate spectrometer equipped with a charge-coupled detector by Raman microscope system and excited by the 514.5 nm (2.41 eV) line of an argon ion laser. Raman spectra of nanotubes under different pressures in the SDAC are plotted in Fig. 1. Spectra are appropriate to SP-SWNT in unloading cycle. Spectrum of SWNT is plotted for comparison. Unfortunately, the 1344 cm^{-1} band of the nanotubes are obscured by the Raman scattering from the diamond anvils for pressure up to 15 GPa. Under more high pressure it is difficult to separate shifted 1594 and 1344 cm^{-1} bands with high enough precision because of lines broadening and low intensity of 1344 cm^{-1} band.

Pressure dependence of diamond Raman band was measured for comparison. First-order Raman spectra was collected from the $5\text{-}\mu\text{m}$ -size region of diamond anvil close to the sample. The experimental procedure is described in detail in Ref. 14.

Hardness measurements of SP-SWNT after pressure treatment were performed using Nanoindentation System (MTS Systems Corporation) equipped with Berkovich diamond in-

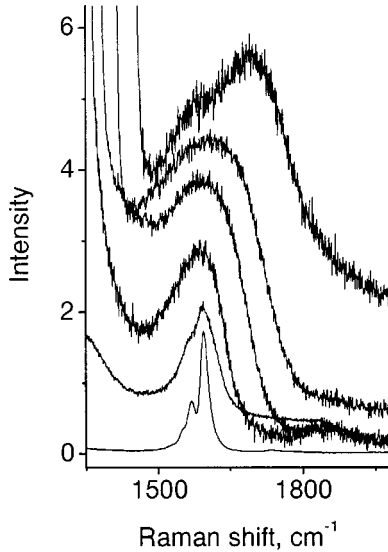


FIG. 1. Raman spectra of SP-SWNT under different pressures in the SDAC (unloading cycle). Appropriate pressures are (starting with top) 55, 36, 18, and 2.5 GPa. Spectra of SP-SWNT (second from bottom) and SWNT (bottom spectrum) are plotted for comparison.

denter. Because of small thickness of sample (about 20 μm) and numerous cracks arose in the sample upon pressure release, the hardness was measured at penetration depth about 40 nm. To increase validity and precision of data, diamond face (100), cubic BN faces (100), and (111) were measured at the same penetration depth for comparison. Force-depth indentation curves of SP-SWNT, diamond face (100), cubic BN faces (100) and (111) and fused silica are plotted in Fig. 2. The possibility and peculiarities for correct hardness measurements of superhard materials at this small penetration depth are discussed in Ref. 15.

The high pressure treatment of the SWNT leads to broadening and redistribution of band intensities in the Raman spectra. Shown in Fig. 3 are spectra appropriate to virgin SWNT [Fig. 3(a)] and to SP-SWNT [Fig. 3(b)]. The spectra of SP-SWNT after unloading do not depend on pressure

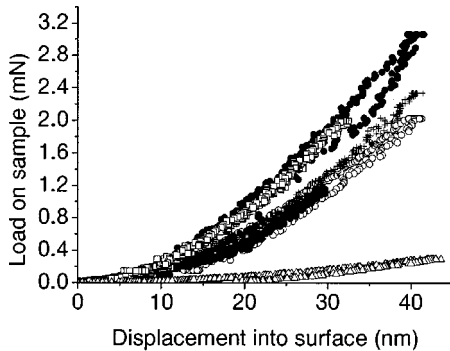


FIG. 2. Force-depth indentation curves of SP-SWNT (marked by solid circles), diamond face (100) (marked by hollow squares) cubic BN faces (100) (marked by hollow circles), and (111) (marked by crosses) and fused silica (marked by hollow triangles) are plotted.

treatment (24 to 55 GPa). It is possible to conclude from the Raman spectra that the nanotubes do not collapse under pressure of at least 55 GPa: since the SWNT band positions are not changed (only are broaden). The peculiarities of spectra also differentiate it from other known types of graphitic and amorphous carbon materials.¹⁶ Because of bands broadening, instead of four bands in the high-frequency region for SWNT [at 1551, 1568, 1592, and 1598 cm^{-1} , Fig. 3(a)] it is possible to resolve only 1561 and 1598 cm^{-1} bands for SP-SWNT using Lorentz multi-peaks fit [Fig. 3(b)]. These bands give maximum at 1594 cm^{-1} in both spectra. The most distinctive evidence of existence of nanotubes after 55 GPa pressure is presence of low-frequency radial breathing mode of SWNT (Ref. 17) at 188 cm^{-1} in the spectra of SP-SWNT [Fig. 3(c)]. The sample was scanned using both micro- and macro-Raman equipment with laser spot size from 1 to 40 μm . In all spectra the band 188 cm^{-1} exists with the same relative intensity. So, we attribute this band to SP-SWNT.

Essential changes in the Raman spectra are associated with the 1344 cm^{-1} band: the relative intensities of the intense bands (188, 1568, 1594, and second-order 2674 cm^{-1}) are the same within 40% after the compression, while the relative intensity of the 1344 cm^{-1} band increased by an order of magnitude. A decreasing of the Raman intensity (by a factor of 2 or more) after relatively low (5.2 GPa) pressure was mentioned in Ref. 18. The second order spectra of SP-SWNT and SWNT are plotted in Fig. 3(d).

There is a direct relationship between the phonon density of states for graphite and SWNT (a nanotube is formed by rolling up a graphene sheet to a cylinder and that gives the possibility of applying the zone-folding method for calculation of the phonon modes of nanotubes¹⁹). On the analogy of transformation of graphite Raman spectrum with decreasing a crystal size^{16,20,21} we attribute the features of SP-SWNT spectra (relative intensities and broadening of the bands 1344, 1568, 1594, 2674, and 2917 cm^{-1}) to the changes of SWNT selection rules. It is important to stress that there are no changes of the band positions of SP-SWNT relative to SWNT (including breathing mode of at 188 cm^{-1}). This fact gives a base to consider SP-SWNT as perturbed SWNT. The formation of superhard phase may occur by internanotube bonding.⁴

The perturbation is possible to attribute to internanotube bonding.⁴ This mechanism is known not only for fullerite⁷ but for graphite sheets, too.²²

Important information about the bulk modulus of SP-SWNT can be derived from the pressure dependence for the modes in high-energy range of the Raman spectra (i.e., the bands around 1590 cm^{-1}). In Fig. 4 the pressure dependence w/w_0 for the $w_0=1594 \text{ cm}^{-1}$ band (as mentioned above, it consists from several bands) is plotted. The bulk modulus B is calculated from the equation $\gamma_i = (B/\omega_i) \partial \omega / \partial P$ (1), where γ_i is the Grüneisen parameter for a quasiharmonic mode of frequency ω_i (Ref. 23). In general, the scaling parameter $\gamma \approx 1$ for the covalently bonding group IV semiconductors²³ and particularly for graphite $\gamma=1.06$ (Ref. 24) to 1.11 (Ref. 25) and for diamond $\gamma=0.96$ (Ref. 26). Recently, the Grüneisen parameter of $\gamma=1.24$ was calculated for SWNT.²⁷ It is important to note, that $\gamma \approx 1$ is expected only for the

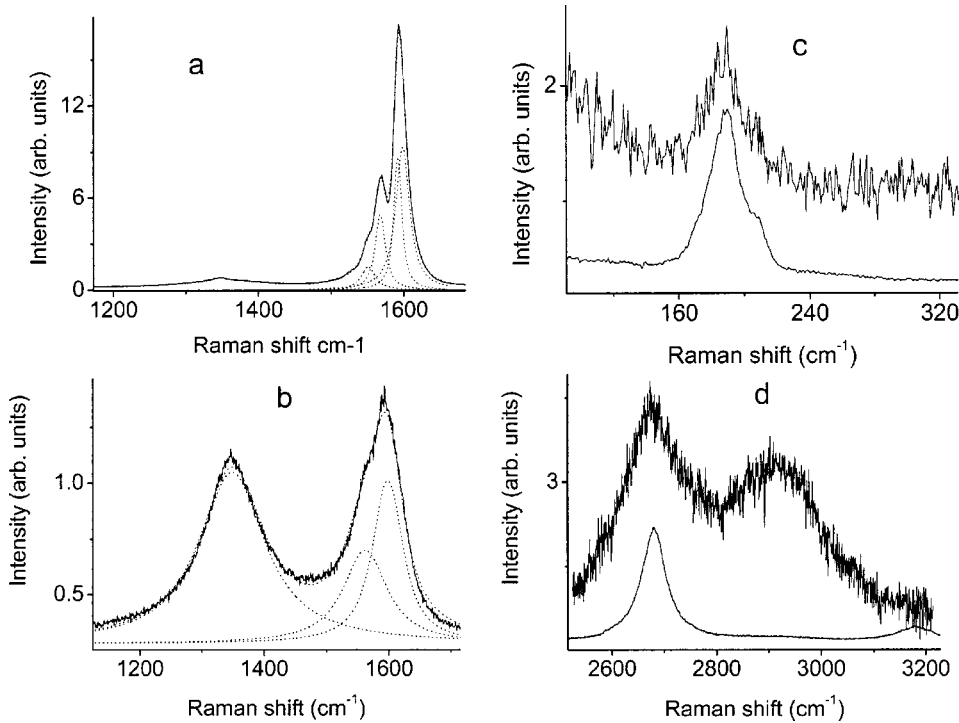


FIG. 3. Raman spectra of SWNT (a), SP-SWNT (b), (c) is low-frequency region of SP-SWNT (overhead) and SWNT (below), and (d) is second-order Raman spectra of SP-SWNT (overhead) and SWNT (below).

mode $\sim 1590 \text{ cm}^{-1}$ that is analogous to the graphite $E_{2g}(G)$ mode. This mode is characteristic of sp^2 bonding.²¹ At the same time for the disorder induced breathing mode of graphite, the $A_{1g}(D)$ band at $\sim 1340 \text{ cm}^{-1}$, $\gamma = 1.9$ according to Ref. 25. The pressure dependence of this mode for the nanotubes also differs from the 1594 cm^{-1} band. Under pressure the mode shifts to a frequency nearer to the characteristic sp^2 band (Fig. 1).

In Fig. 4, the pressure dependence of the 1594 cm^{-1} band is plotted over the entire pressure range. Data appropriate to SWNT and the first and second SWNT phases are marked by hollow circles. Changes in slope (hollow circles) indicate phase transitions at pressures of 14 ± 1 , 19 ± 1 , and 24 ± 1 GPa. The pressure dependence about $6 \text{ cm}^{-1}/\text{GPa}$ for SWNT 1594 cm^{-1} band under pressure below 14 GPa is consistent with data reported in Ref. 28 for SWNT ($5.7 \text{ cm}^{-1}/\text{GPa}$): the shift agrees with the pressure dependence of the high-energy modes of isolated nanotubes under compression.^{18,28}

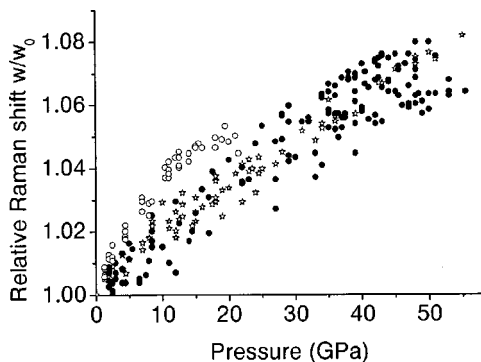


FIG. 4. The pressure dependence of the 1594 cm^{-1} band of SWNT (hollow circles), SP-SWNT (solid circles), and diamond (stars).

For determination of bulk modulus of SP-SWNT, we have used data appropriate to sample treated by pressure above 25 GPa and shear deformation. These data are marked by solid circles in Fig. 4. No hysteresis is seen in the pressure dependence of SP-SWNT. This is direct evidence that transformation of the nanotubes is irreversible.

Pressure dependence of w/w_0 for diamond Raman band $w_0 = 1333 \text{ cm}^{-1}$ measured at the same conditions is plotted in Fig. 4 for comparative study of bulk modulus. Appropriate to diamond points are marked by stars. Accidentally, the pressure dependence for the diamond and the SP-SWNT Raman bands are very similar with high accuracy in Fig. 4. In this case bulk modulus of SP-SWNT, B_s is proportional to that of diamond B_d : $B_s = \gamma_s/\gamma_d B_d$ from Eq. (1) where γ_s is Grüneisen parameter for SP-SWNT and γ_d is diamond Grüneisen parameter. Consequently, the bulk modulus of SP-SWNT exceeds bulk modulus of diamond 1.1 to 1.3 times, depending on choice of γ : experimental data for graphene sheet or calculated value for SWNT.

According to Ref. 29 bulk module of single diamond crystal is 420 GPa. Thus, for SP-SWNT bulk module is 462 to 546 GPa.

Hardness measurements of SP-SWNT were performed using Nanoindentation System. To increase precision and validity of hardness data, a procedure of calibration against material with known hardness (standard) was used. This procedure was elaborated in detail in Refs. 8, 30, and 31. Nitrogen-free diamond single crystal³¹ [face (100)], 1-mm-size cubic BN single crystals [faces (100) and (111) (Ref. 32)] and fused silica were used as standard materials. By definition hardness (H) is calculated with the relation $H = P/S$. P is load to the indenter and S is the projected area of contact. If we compare indentations in different materials (with hardness H_1 and H_2) with the same value of S (or

penetration depth using the same indenter), then $H_1 = (P_1/P_2)H_2$, where P_1 and P_2 are appropriate loads on indenter. Results of hardness measurements of SP-SWNT, diamond, *c*-BN and fused silica are plotted in Fig. 2.

Hardness calibration measurements of *c*-BN and fused silica were performed at indentation depth about 1 μm . The hardness values are *c*-BN (111) are 66 ± 1 to 73 ± 1 GPa depending on orientation of indenter relative to crystallographic axis of sample (so-called hardness anisotropy); *c*-BN (100) is 62 ± 1 GPa [effect of anisotropy for the Berkovich indenter is not so strong as for (111) face]; fused silica is 12 ± 0.5 GPa. According to recent data³¹ hardness of nitrogen-free diamond [face (100)] belongs to the range 140 to 160 GPa depending on anisotropy hardness effect. Since three-sided pyramidal Berkovich indenter is not sensitive to anisotropy in cubic (100) face, we use for estimation of hardness average value 150 GPa.

All calibration measurements were performed with optical polish quality of surfaces including diamond (we have used a diamond anvil). Because sample of SP-SWNT was synthesized using flat diamond anvils, no special preparation is necessary for hardness measurements of the sample.

Hardness data of SP-SWNT reveal large scattering. Possible reasons of the scattering are both structure heterogeneity and microcracks in the sample. As the sample was formed under high pressure and upon unloading, large internal

stresses can lead to cracking. Removing detailed statistic analysis of hardness to our future publications, we report in the present manuscript only range of hardness (minimum and maximum hardness) for SP-SWNT. Especially the result is graphic: minimum SP-SWNT hardness appropriate to *c*-BN while maximum hardness appropriate to diamond.

Load-displacement curves for SP-SWNT appropriated to the confines of the range are plotted in Fig. 2. The lower curve of SP-SWNT (minimum hardness) corresponds with the curve of *c*-BN face (100) and upper corresponds with nitrogen-free diamond [face (100)]. Hence, the hardness of SP-SWNT belongs to the range 62 to 150 GPa and permits us to attribute SP-SWNT to the class of superhard materials.

High mechanical properties of SP-SWNT, namely, bulk modulus (462 to 546 GPa) exceeding or comparable with diamond and hardness (62 to 150 GPa) belongs to the range between cubic BN and diamond, preservation of Raman bands of SWNT in SP-SWNT along with the bands broadening and absence of new bands (within the detection limit), are characteristic for the new phase.

This work was supported by the Frontier Carbon Technology Project, which was consigned to JFCC by NEDO. We thank Dr. T. Taniguchi for samples of cubic BN and Dr. Y. Ohkubo (JASCO) for providing us with preliminary Raman measurements.

-
- ¹S. Iijima and T. Ichihashi, *Nature (London)* **363**, 603 (1993).
²D. H. Robertson, D. W. Brenner, and J. W. Mintmire, *Phys. Rev. B* **45**, 12 592 (1992).
³M. M. J. Treacy, T. W. Ebbesen, and J. M. Gibson, *Nature (London)* **381**, 678 (1996).
⁴L. A. Chernozatonskii, *Chem. Phys. Lett.* **297**, 257 (1998).
⁵V. Blank *et al.*, *Phys. Lett. A* **188**, 281 (1994).
⁶V. Blank *et al.*, *Phys. Lett. A* **205**, 208 (1995).
⁷V. Blank *et al.*, *Carbon* **36**, 319 (1998).
⁸V. Blank, M. Popov, G. Pivovarov, N. Lvova, K. Gogolinsky, and V. Reshetov, *Diamond Relat. Mater.* **7**, 427 (1998).
⁹R. S. Ruoff and A. L. Ruoff, *Nature (London)* **350**, 663 (1991).
¹⁰A. M. Rao *et al.*, *Science* **259**, 955 (1993).
¹¹A. F. Goncharov, *Sov. Phys. JETP* **71**, 1025 (1990).
¹²V. V. Aksenonkov, V. D. Blank, N. F. Borovikov, V. G. Danilov, and K. I. Kozorezov, *Phys. Dokl.* **39**, 700 (1994).
¹³A. G. Rinzler *et al.*, *Appl. Phys. A: Mater. Sci. Process.* **67**, 29 (1998).
¹⁴M. Hanfland and K. Syassen, *J. Appl. Phys.* **57**, 2752 (1985).
¹⁵A. Richter *et al.*, *Diamond Relat. Mater.* **9**, 170 (2000).
¹⁶D. S. Knight and W. B. White, *J. Mater. Res.* **4**, 385 (1989).
¹⁷A. M. Rao *et al.*, *Science* **275**, 187 (1997).
¹⁸U. D. Venkateswaran *et al.*, *Phys. Rev. B* **59**, 10 928 (1999).
¹⁹R. Al-Jishi, L. Venkataraman, M. S. Dresselhaus, and G. Dresselhaus, *Chem. Phys. Lett.* **209**, 77 (1993).
²⁰R. J. Nemanich and S. A. Solin, *Phys. Rev. B* **20**, 392 (1979).
²¹A. C. Ferrari and J. Robertson, *Phys. Rev. B* **61**, 14 095 (2000).
²²V. Blank *et al.*, *Diamond Relat. Mater.* **8**, 1285 (1999).
²³B. A. Weinstein and R. Zallen, in *Light Scattering in Solids*, edited by M. Cardona and G. Guntherodt (Springer, Berlin, 1984), Vol. IV.
²⁴M. Hanfland, H. Beister, and K. Syassen, *Phys. Rev. B* **39**, 12 598 (1989).
²⁵A. F. Goncharov and V. D. Andreev, *Sov. Phys. JETP* **73**, 140 (1991).
²⁶M. Hanfland, K. Syassen, S. Fahy, S. G. Louie, and M. L. Cohen, *Phys. Rev. B* **31**, 6896 (1985).
²⁷S. Reich, H. Jantoljak, and C. Thomsen, *Phys. Rev. B* **61**, 13 389 (2000).
²⁸C. Thomsen *et al.*, *Appl. Phys. A: Mater. Sci. Process.* **69**, 309 (1999).
²⁹V. M. Prokhorov, V. D. Blank, S. G. Buga, and V. M. Levin, *Synth. Met.* **103**, 2439 (1999).
³⁰V. Blank, M. Popov, N. Lvova, K. Gogolinsky, and V. Reshetov, *J. Mater. Res.* **12**, 3109 (1997).
³¹V. Blank, M. Popov, G. Pivovarov, N. Lvova, and S. Terentev, *Diamond Relat. Mater.* **8**, 1531 (1999).
³²T. Taniguchi and S. Yamaoka, *J. Cryst. Growth* **222**, 549 (2000).